Official URL : https://doi.org/10.1016/j.nima.2009.05.078

To cite this version :

Goiffon, Vincent and Magnan, Pierre and Saint-Pé, Olivier and Bernard, Frédéric and Rolland, Guy Ionization versus displacement damage effects in proton irradiated CMOS sensor manufactured in deep submicron process. (2009) In: 5th International Conference on New Developments In Photodetection (NDIP08), 15 June 2008 - 20 June 2008 (Aix-les-Bains, France).

Ionization versus displacement damage effects in proton irradiated CMOS sensors manufactured in deep submicron process

V. Goiffon [a,*], P. Magnan [a], O. Saint-Pé [b], F. Bernard [c], G. Rolland [c]

[a] Université de Toulouse, ISAE, 10 ave. E. Belin, 31055 Toulouse, France
[b] EADS Astrium, 31 ave. des cosmonautes, 31402 Toulouse, France
[c] CNES, 18 ave. E. Belin, 31401 Toulouse, France

A R T I C L E I N F O

Keywords:
CMOS image sensors
Active pixel sensors
APS
Proton irradiation
Shallow trench isolation
Dark current

A B S T R A C T

Proton irradiation effects have been studied on CMOS image sensors manufactured in a 0.18 μm technology dedicated to imaging. The ionizing dose and displacement damage effects were discriminated and localized thanks to ^{60}Co irradiations and large photodiode reverse current measurements. The only degradation observed was a photodiode dark current increase. It was found that ionizing dose effects dominate this rise by inducing generation centers at the interface between shallow trench isolations and depleted silicon regions. Displacement damages are is responsible for a large degradation of dark current non-uniformity. This work suggests that designing a photodiode tolerant to ionizing radiation can mitigate an important part of proton irradiation effects.

1. Introduction

The use of CMOS image sensors (CIS) in space applications will considerably grow in the future [1]. Space radiation tolerance of tomorrow's CMOS imagers is therefore a primary concern for scientists and engineers designing imaging systems. Previous works have already focused on γ-radiation effects on sensors manufactured in deep submicron CIS technology [2,3]. We present here a study of proton irradiation effects on deep submicron CMOS imagers through the discrimination of ionization effects and displacement damage effects. This was done thanks to the comparative study of several isolated photodiodes for several proton energies and fluences.

This paper deals only with dark current increase since the other sensor characteristics, such as the photo-response or MOSFETs *I–V* characteristics, were not degraded by the irradiation. Proton irradiation also induced random telegraph dark current fluctuations which will be studied later.

2. Experimental

In order to discriminate area and perimeter dependent dark current contributions, we designed rectangular photodiodes with various area over perimeter ratios. On the same die, we also designed an array constituted by 128 × 128 pixels with three NMOS transistors and one photodiode per pixel. The pixel pitch is 10 μm and the photodiode size is about 9.2 μm × 8.1 μm. These integrated circuits were manufactured thanks to a 0.18 μm CMOS process dedicated to imaging (CIS). In this technology, photodiodes are formed by an optimized lightly doped N deep diffusion in a lightly doped P epitaxial layer. The N region is surrounded by shallow trench isolation (STI) oxides. The lateral depletion region is in direct contact with the STI.

Current–voltage characterizations were carried out thanks to a dedicated low current test bench described in Ref. [3]. The pixel array was operated in hard reset mode by applying 2.4 V on the reset MOST drain whereas the operating voltage was set to 3.3 V.

Proton irradiation took place at the Kernfysisch Versneller Instituut (KVI), Netherlands, the Université catholique de Louvain (UCL), Belgium, and Isotron, UK. The irradiation details are summarized in Table 1. Measurements were performed at 296.15 K and post-irradiation characterizations were carried out between one and two months after exposure to proton beams. In order to estimate ionizing dose, linear energy transfer (LET) from SRIM was used whereas displacement damage dose and damage factors were estimated thanks to non-ionizing energy loss (NIEL) values from Ref. [4].

3. Results and discussion

3.1. Photodiodes

Only the photodiodes of circuit numbers 1–3 were characterized. Reference photodiode reverse current evolution with reverse

* Corresponding author. Tel.: +33 5 61338251; fax: +33 5 61338345.
E-mail address: vincent.goiffon@isae.fr (V. Goiffon).

bias is shown before and after proton irradiation in Fig. 1. The area over perimeter ratio of these photodiodes, $A/P = 2.5\,\mu m$, is quite close to the pixel array photodiode one. Therefore, the $2000 \times 5\,\mu m^2$ photodiodes results are thought to be representative of in-pixel photodiode behaviors. A significant rise is observed after irradiation on the current and its slope, indicating an increase of the number of generation centers in the photodiode depletion region. Dark current as a function of photodiode perimeter is presented in Fig. 2 for 2.4 V reverse voltage. The diode area is fixed to $10^4\,\mu m^2$. The perimeter clearly plays an important role in dark current. Before irradiation, this is explained by a much higher defect density at the silicon–STI interface than in the bulk [5]. After exposure to proton beams, both perimeter and bulk dark currents are greatly enhanced. Bulk generation centers are created by displacement damages and the relationship between displacement damage dose D_{dd} and mean dark current increase ΔI_{dark} has been experimentally established in silicon photodetector [6]: $\Delta I_{dark} = qV_{dep}D_{dd}K_{dark}$, where q is the elementary charge, V_{dep} the depleted volume and K_{dark} the universal factor equals $(1.9 \pm 0.6) \times 10^5$ carriers $cm^{-3}\,s^{-1}$ per MeV/g at 300 K. The comparison between this factor and our data is presented in Fig. 3. It shows the estimated damage factor as a function of area over perimeter ratio with and without the perimeter dark current contribution. The error bars only take into account measurement noise and correlation between our data and the linear regressions used to estimate the damage factor. Photodiodes with the highest area over perimeter (A/P) ratios give a damage factor in very good agreement with previous work, whereas the photodiodes with $A/P = 2.5\,\mu m$ yield an extremely large value. This is obviously caused by the perimeter contribution, and when this contribution is subtracted from the measurement, the results are in much better agreement with the universal factor. Therefore, displacement damages in these photodiode depleted volumes correspond well with the literature, whereas the perimeter dependent contribution is much higher than what can be explained by displacement damage alone. An electric field enhancement effect localized along the diode perimeter could be the cause of this unexpected effect. However, high electric field is not likely in these lightly doped optimized photodiodes and Fig. 1 does not exhibit a significant electric field enhancement [7].

Hence, this peripheral dark current increase is most likely due to ionization effects. This agrees with the degradation observed after ^{60}Co irradiation of the same devices [3].

Table 1
Irradiation details.

IC #	Facility	Energy (MeV)	Fluence (cm^{-2})	TID (Gy)	DDD (TeV/g)	DC pre/post (fA)
1*	KVI	50	8.8×10^9	14	34.2	0.14/0.58
2*	KVI	100	1.5×10^{10}	14	38.9	0.14/0.51
3*	KVI	184	2.4×10^{10}	14	48.3	0.16/0.61
4	KVI	50	2.0×10^{10}	32	77.6	0.14/1.07
5	KVI	50	5.0×10^9	8	19.4	0.14/0.43
6	Isotron	7.4	3.2×10^9	22	31.6	0.15/0.59
7	UCL	9.3	1×10^{10}	59	83.2	0.21/1.11
8	UCL	62	3×10^{11}	402	1022.8	0.25/12.1
9	UCL	62	1×10^{11}	134	340.9	0.18/3.94

TID and DDD stand for total ionizing dose (in Gy(Si)) and displacement damage dose, respectively. DC pre/post means dark current measured on pixel arrays before and after proton irradiation. Circuit numbers with an * indicate that isolated photodiodes have been characterized on these circuits.

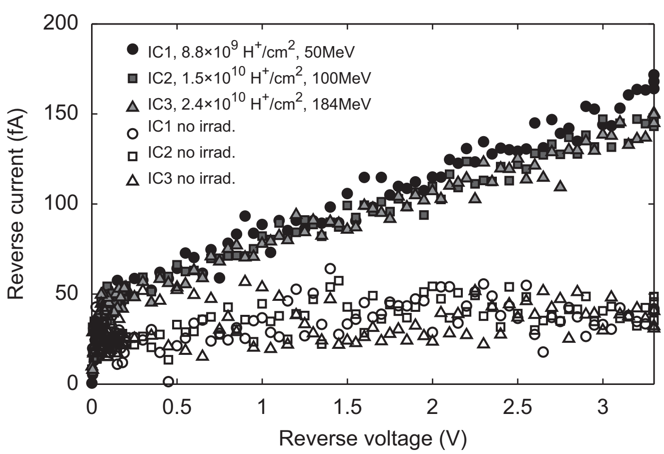

Fig. 1. Reverse current–voltage characteristics of reverse biased $2000 \times 5\,\mu m^2$ photodiodes before and after proton irradiation.

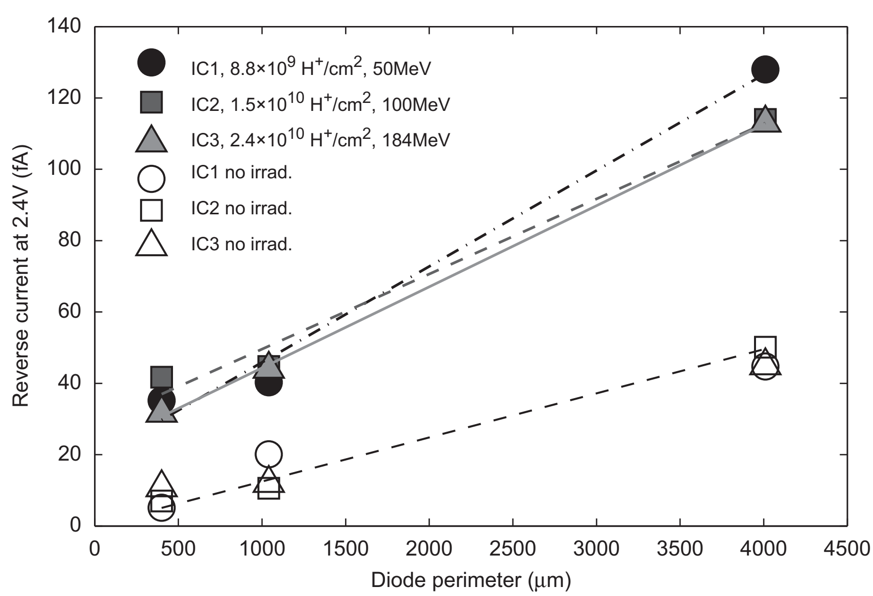

Fig. 2. Photodiode dark current versus perimeter. The devices were reverse biased at 2.4 V. The photodiode areas are equal to $10^4\,\mu m^2$.

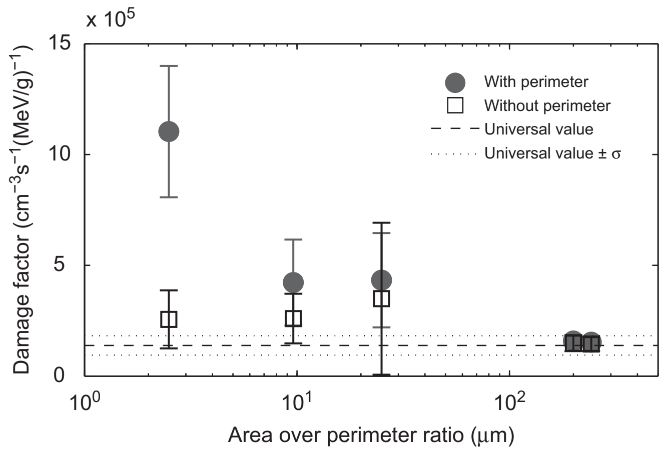

Fig. 3. Displacement damage factor with and without the perimeter contribution. The universal damage factor at 296.15 K is also plotted with its standard deviation.

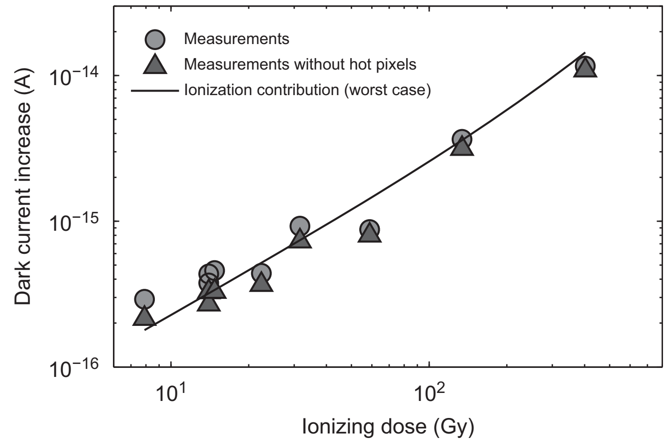

Fig. 5. Comparison between measured mean dark current increase and estimated ionization contribution. The mean dark current without hot pixel contribution is also shown for a better comparison with ionizing dose effects.

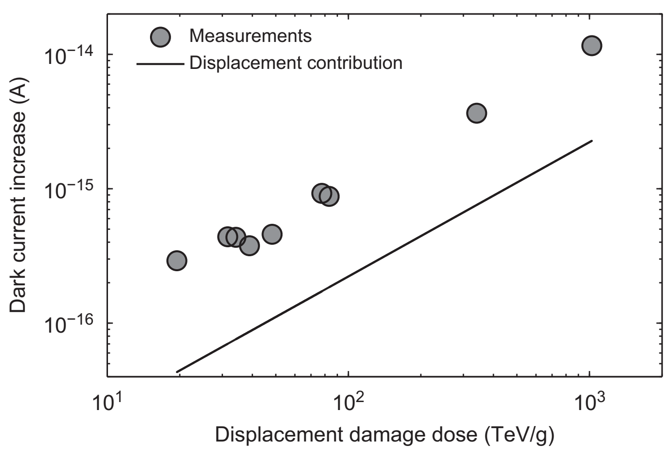

Fig. 4. Comparison between measured mean dark current increase and estimated displacement damage contribution. This contribution was estimated thanks to the universal damage factor [6].

3.2. *Pixel arrays*

The mean dark current increase, i.e. the difference between pre- and post-irradiation mean dark currents, is plotted as a function of the displacement damage dose in Fig. 4. Whatever the facility, the fluence, or the proton energy used, the results seem consistent. The mean dark current increase due to displacement damage in the depleted volume was estimated thanks to the universal damage factor at 296.15 K, extrapolated with a 0.63 eV activation energy. The depleted volume is not known precisely, and a worst case estimation was used for the calculation. This displacement dark current is plotted as a solid line in the figure. As expected from isolated photodiode results, measured dark current increase is much greater than the NIEL induced dark current.

The same comparison with estimated ionization effects is presented in Fig. 5. This approximation is based on ^{60}Co 1.17 and 1.33 MeV γ-ray irradiation results [3], which have been interpolated thanks to a second order polynomial function. This estimation represents a worst case regarding the proton irradiation. Firstly, because ^{60}Co gamma radiation is known to have a higher fractional yield than particles with higher LET [8]. Secondly, these measurements were performed less than 24 h after exposure to ^{60}Co whereas room temperature annealing should have occurred on proton irradiated devices during the storage time. Nevertheless, despite these approximations, Fig. 5 clearly shows that ionization can easily dominate the dark current increase, as it was concluded in the previous section. This is especially true when hot pixels, mainly due to displacement damages, are rejected for the mean computation, as shown by the triangle markers in the figure.

In order to reveal a possible electric field enhancement, the IC1 dark current activation energy versus dark current is shown before and after proton irradiation in Fig. 6. The correlation between high dark current pixels and low activation energy (below midgap) suggests a slight electric field enhancement [9] on the unirradiated device (Fig. 6(a)). After irradiation (Fig. 6(c)), the mean activation energy rises from 0.61 to 0.64 eV. It corresponds well to the 0.63 eV value usually observed in irradiated devices [6,10,11] and the correlation between dark current value and activation energy vanishes. Indeed, pixels with the highest dark currents mainly have activation energies above midgap and the number of pixels with activation energies below midgap is negligible. Thus, electric field enhancement does not seem to play a significant role in the unexpected large dark current values. On the other hand, activation energies after proton irradiation tend to align on the mean value. The same phenomenon is observed on ^{60}Co irradiated devices, especially at high ionizing doses (Fig. 6(b)), when the dominant defects are ionization induced generation centers located at the STI interface. This is consistent with a dominant ionization induced dark current. It can also be inferred from Fig. 6(b) that electric field enhancement is a negligible process at the STI interface. However, electric field enhancement can still exist in the depleted volume but it would be masked by the dominant interface effects.

Fig. 7 shows the dark current distribution of two irradiated sensors compared to non-uniformity induced by ionization. Like for the mean dark current increase, the ionization contribution to the dark current standard deviation was estimated by a polynomial function. This figure clearly shows that whereas displacement damages have a negligible influence on the mean dark current increase, they play a significant role in the dark current uniformity degradation. The same trend was observed after each proton irradiation: measured standard deviation was roughly three times larger than the one estimated by estimation based on ionizing dose effects.

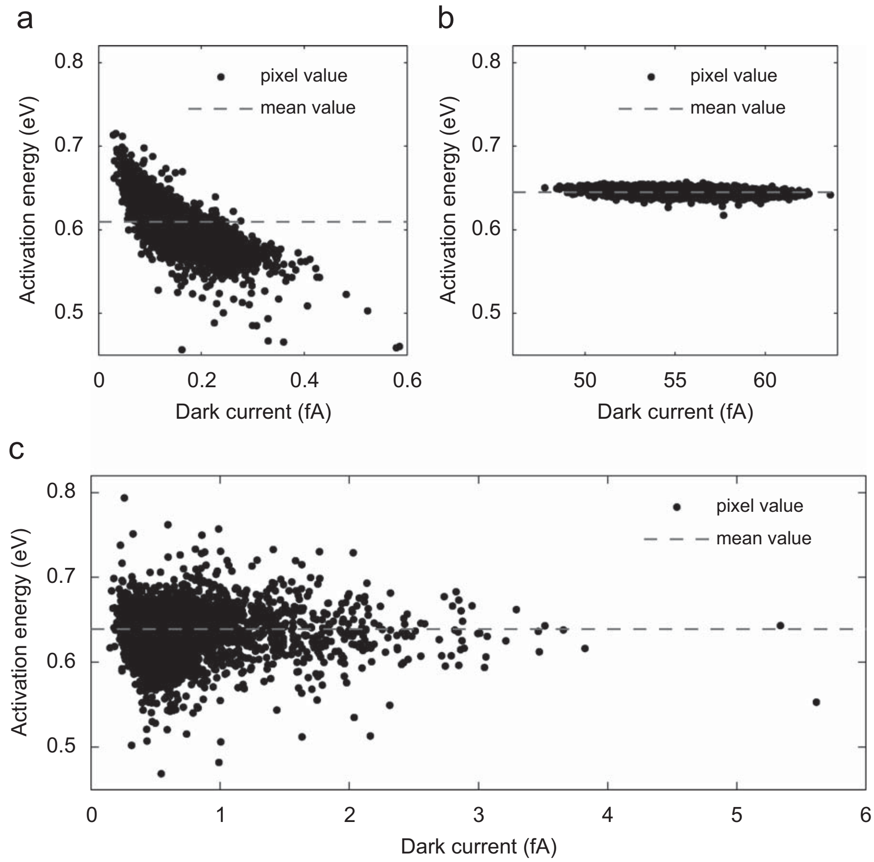

Fig. 6. IC1 dark current activation energy versus dark current at 296.15 K (a) before and (c) after 50 MeV H^+ irradiation. Activation energies estimated on a device irradiated by ^{60}Co up to 1 kGy are also shown (b).

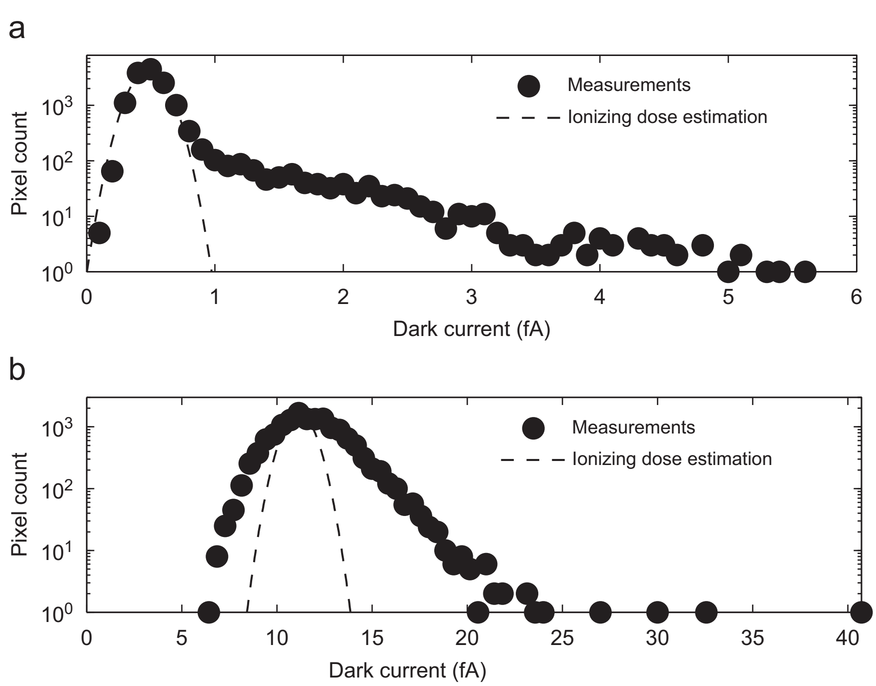

Fig. 7. Dark current distribution of IC1 irradiated by 50 MeV at 8.8×10^9 H^+/cm^2 and IC8 irradiated by 62 MeV at 3×10^{11} H^+/cm^2. An estimation of ionization induced dark current non-uniformity is also plotted.

4. Summary and conclusion

Up to 1 PeV/*g* displacement damage dose, proton irradiations have only induced dark current rises in the tested CMOS image sensors. We showed that these rises were mainly due to an increase of the number of generation centers at the interface between photodiode depletion regions and shallow trench isolations. Since ionizing energy loss is responsible for generating these defects, the main part of proton irradiation effects can be consequently reduced by using ionizing dose hardened photodiodes for CMOS sensor design. This can be done by changing the photodiode surrounding environment [12].

Non-ionizing energy loss was also seen to have an impact on sensor performances by inducing significant dark current non-uniformities. Displacement damage contribution to mean dark current increase agreed well with the universal damage factor but this effect was negligible in front of ionization effects in pixel photodiodes. Future work will focus on designing ionization hard CMOS sensors for studying more precisely proton induced displacement damage effects.

Acknowledgments

Proton irradiation opportunities offered by Ludovic Duvet from ESA, Françoise Bezerra and Sophie Petit from CNES, Gordon Hopkinson from SSTL and Thierry Nuns from ONERA are gratefully acknowledged. The authors also thank Christiane Duprat from INSA-AIME, Céline Engel, Paola Cervantes, Philippe Pinel, Franck Corbière and Nicolas Huger from ISAE for their help with circuit design, packaging and experimental issues.

References

[1] L. Duvet, D.D.E. Martin, A. Owens, Proc. SPIE 6276 (2006) 627606.
[2] P.R. Rao, X. Wang, A.J. Theuwissen, Solid-State Electron., 52 (9) (2008) 1407.
[3] V. Goiffon, P. Magnan, O. Saint-Pé, F. Bernard, G. Rolland, IEEE Trans. Nucl. Sci. NS-55 (6) (2008) 3494.
[4] C. Dale, P. Marshall, B. Cummings, L. Shamey, A. Holland, IEEE Trans. Nucl. Sci. NS-40 (6) (1993) 1628.
[5] S. Inaba, M. Takahashi, Y. Okayama, A. Yagishita, F. Matsuoka, H. Ishiuchi, in: Symposium on VLSI Technology, 1997, p. 2584.
[6] J.R. Srour, D.H. Lo, IEEE Trans. Nucl. Sci. NS-47 (6) (2000) 2451.
[7] M.J.J. Theunissen, Solid-State Electron. 28 (1985) 417.
[8] T.R. Oldham, J.M. McGarrity, IEEE Trans. Nucl. Sci. NS-30 (1983) 4377.
[9] J.R. Srour, R.A. Hartmann, IEEE Trans. Nucl. Sci. NS-36 (6) (1989) 1825.
[10] J.R. Srour, S.C. Chen, S. Othmer, R.A. Hartmann, IEEE Trans. Nucl. Sci. NS-25 (1978) 1251.
[11] G.R. Hopkinson, IEEE Trans. Nucl. Sci. NS-39 (6) (1992) 2018.
[12] B.R. Hancock, T.J. Cunningham, K.P. McCarty, G. Yang, C.J. Wrigley, P.G. Ringold, R.C. Stirbl, B. Pain, Proc. SPIE 4306 (2001) 147.